ISSN 1064-2293, Eurasian Soil Science, 2021, Vol. 54, No. 9, pp. 1385–1399. © Pleiades Publishing, Ltd., 2021.
Russian Text © The Author(s), 2021, published in Pochvovedenie, 2021, No. 9, pp. 1097–1112.

TOMOGRAPHY OF SOIL PORE SPACE

Tomography in Soil Science: From the First Experiments to Modern Methods (A Review)

K. N. Abrosimov[a, *], K. M. Gerke[b], D. S. Fomin[a], K. A. Romanenko[a], and D. V. Korost[a, c]

[a] *Dokuchaev Soil Science Institute, Russian Academy of Sciences, Moscow, 119017 Russia*
[b] *Schmidt Institute of Physics of the Earth, Russian Academy of Sciences, Moscow, 123242 Russia*
[c] *Lomonosov Moscow State University, Moscow, 119991 Russia*
**e-mail: abrosimov_kn@esoil.ru*

Received February 4, 2021; revised March 29, 2021; accepted April 7, 2021

Abstract—The article provides an overview of the use of computed tomography in the study of soils from the first works to the present time. The development of computed tomography in the field of hardware and methods for processing tomographic data—from the first attempts to analyze soil structure using tomographic sections of low quality to modern methods of segmentation and analysis of volumetric structures using specialized software, correlation functions and neural networks—is discussed. The purpose of the article is to show the possibilities of methods for processing tomographic data in relation to studies of soil structure and to analyze possible trends of their further development. The article presents examples from the world experience of using computed tomography for a broad variety of soils, shows various methods of data segmentation that have been used from the first studies to the recent ones. The specific terminology coined in the course of the evolution of the method and various morphometric indicators for 2D and 3D images are presented, and a forecast of the prospects for the method in the near future is given.

Keywords: XCT, image analysis, pore space, soil structure, tomographic studies, mCT
DOI: 10.1134/S1064229321090027

INTRODUCTION

Computed tomography (CT) is an actively developing method in soil science. From the moment of its appearance until the beginning of the 21st century. this method was poorly demanded by soil scientists. Most of the published studies were limited to tomographic imaging of large cylindrical specimens—undisturbed soil cores ("soil monoliths"). Computed tomography was applied in studies of soil bulk density [69], structure of large pores of zoogenic origin [13, 46], soil water content [5, 17], and the spatial distribution of moisture in the soil [6].

The physical basis of the method is the exponential law of radiation attenuation. In the X-ray range, the exponential law is fulfilled with a high degree of accuracy; therefore, the developed mathematical algorithms were first applied specifically for X-ray computed tomography. In 1963, the American physicist A. Cormack solved the problem of tomographic image reconstruction [16], and in 1969 the English engineer-physicist G. Hounsfield from EMI Ltd designed an EMP scanner [42]—the first computerized X-ray tomograph, clinical trials of which took place in 1971.

The reorientation of computer manufacturers to the private user, the ubiquity of personal computers and the growth of their productivity, the development of microelectronics for the entertainment industry—exerted a positive impact on the development of many industries, including the launch of mass production of X-ray tomographs of a completely new type: small in size, structurally simple, and allowing one to study the microstructure of small objects with high resolution. 3D structure analysis has become available to almost anyone. This also influenced the possibilities of studying the structure of soils.

In the first tomographic studies [17, 69], it was possible to consider only large objects or macropores in the volume of a soil sample. The development of the technological base made it possible to move to a different level of research accuracy: 3D studies of soil at the meso, micro, and nano levels. The parallel development of methods for image analysis made it possible to determine the most convenient algorithms for segmentation of X-ray contrast phases and to develop programs for calculating volumetric parameters based on segmented data. In many ways, automatic algorithms are imperfect. Automatic segmentation is still not reliable [4] and is used to a limited extent. So far, there is no possibility of classifying objects of the same phase by their genesis (for example, dividing the pore space into channels and fissures), but there is a possi-

bility of separating soil pores according to their shape and orientation in space.

The hardware and mathematical capabilities of tomography, as well as the tasks of soil research (analysis of the internal structure and various natural processes, the growth and development of the root system, compaction, changes during the application of fertilizers, etc.) have shaped the appearance of modern tomographic soil research, as well as the methods of tomographic research. In modern tomographic research, the soil can be studied in several ways at once:

(1) **In soil cores (monoliths).** A core sample of undisturbed soil (soil monolith) for tomographic research is somewhat different from the usual soil core sample for a soil scientist. This is the soil sampled into an X-ray transparent tube (PVC tube) of cylindrical shape with a diameter of 5 to 20 cm and a height of up to 1 m. This shape of the sample is used for studies of various practical directions: the study of soil macroporosity [70], the development of root systems [63] or zoogenic pores [13, 14], changes in the structure of soil and soil pore space upon application of mineral fertilizers [107], studies of soil degradation and compaction [35], and the influence of various soil factors on the absorption coefficient of X-ray radiation [97]. From the 1980s to the present, the structure of soils has been studied in this way with a low resolution because of limitations of the equipment. There are no specialized tomographs for the study of soils in the world. Most of the research is carried out on medical (various Siemens models: Somatom 64, Plus, 512CR, Philips Tomoscan, etc.), industrial (SMS Model 101B+ CITA), or geological (Russian RKT-180 and its foreign analogues) tomographs, where the resolution is no higher than 70 microns. However, at the beginning of 2010, microtomographs that made it possible to scan a fragment of a monolith of 10 cm in diameter and 15–20 cm in height with a resolution of about 10 μm appeared on the market (Bruker SkyScan 1073, 1273, 2211, 2214 and Nikon and GE models close to them in terms of parameters), which opened up new possibilities for studying the structure of soil and soil pore space at the macro- and mesolevels.

(2) **In small soil cores (micromonoliths).** The term *micromonolith* is only used in Russian soil science [4, 32] and nowhere else, but soil cores of comparable shape and size with slight differences are used everywhere in research. Micromonolith is a cylindrical soil sample packed in a plastic X-ray transparent cylinder. In shape, it is a reduced version of a monolith of up to 1–3 cm in diameter and 5 cm in height. The tasks of studying soils in such cores include everything the same as for monoliths. But where detailed resolution is required, it is possible to analyze the structure at the meso- or microlevel. So, micromonoliths are used for a step-by-step study of the development of the root system [51, 63, 95], tracking structural changes during swell–shrink [91, 92] and freezing–thawing [39, 83, 99] processes, anthropogenic soil compaction, and in a number of other studies [7, 9, 35, 53, 55, 73, 74, 84, 90]. The resolution of the tomographic survey for micromonoliths is slightly different depending on the equipment used (tomograph) and the diameter of the micromonolith and can vary from 1 to 30 microns. Micromonoliths can be scanned on medical tomographs, but samples of this size will not be representative, since most of the microdetails will simply be lost because of the low resolution.

(3) **In soil aggregates.** A soil aggregate is a natural complex soil unit composed of microaggregates and/or elementary soil particles [3]; it is a very convenient object for investigation by the method of computed microtomography. Most of the aggregates are characterized by low absorption of X-ray radiation and overall dimensions that are convenient for tomographic examination in the range of 1–4 μm. In aggregates with a fractional size of 3–5 mm and less, the study of the inner structure and intra-aggregate porosity is difficult or even impossible by traditional methods of micromorphology (thin sections, polished sections). Modern microtomographs make it possible to study the structure of individual aggregates with a fractional size of up to 500 μm with a resolution of 750 (Bruker SkyScan 1172) or 60 nm (Bruker SkyScan 2214). In the future, in addition to studying the microporosity of soils [94], it will be possible to move to the level of nanoporosity of microaggregates by combining the data of tomography and electron microscopy. The first works in this direction are already underway [31].

The main advantage of the computed tomography method is a nondestructive nature of this method with an accurate reconstruction of the volumetric structure consisting of contrasting phases visible in X-rays: the solid phase of the soil, pore space, and organic objects (roots, organic residues, etc.). The advantages of tomography in comparison with traditional morphological and micromorphological methods are: (1) the high speed of obtaining results, including the ability to conduct accurate 3D monitoring of changes in the soil structure, moisture, and other parameters with a high resolution (up to 1 micron and less) and (2) noninvasiveness (the study takes place without changing the structure and properties of the sample) [32]. With the help of tomographic imaging, it is possible to study soil samples at different moisture levels—from completely water-saturated to dry—and at different temperatures, including the frozen state [83, 92]. This enables a step-by-step study of the dynamics of changes in the structure (microstructure) of the pore space of soils.

In addition to the methods soil tomography, the development of methods for obtaining and processing tomographic data is of interest. If 2D analysis has remained virtually unchanged since the 1980s and is used in this form for the analysis of tomographic slices [9, 93], then 3D analysis is developing very intensively.

The disadvantages and limitations of the method do not seem obvious, but they are significant: (1) the volume of tomographic data depends on the sample size and resolution; (2) the presence of intersection of X-ray contrast phases of different minerals in gray-scale (or the problem of partial filling of a pixel/voxel). which complicates the identification of individual mineral phases in the sample, but can be solved by comparing thin sections and tomographic sections; (3) the need in human intervention at the stages of phase segmentation and software processing (filtering) of tomographic images; and (4) imperfection of methods for analyzing volumetric structures in soil. Criteria for assessing the state of soils at different levels of structural organization are only at the stage of elaboration, as well as some volumetric indicators by which these soils are supposed to be assessed. It should be noted that most of the listed disadvantages are not inherent to the method itself and do not have a fundamental nature; it can be supposed that they will be minimized or eliminated in the future.

MACROTOMOGRAPHY OF SOILS. FIRST EXPERIMENTS, 1980–2000

Possibilities and limitations of soil macrotomography. In the first years of the development of soil tomography, soils were studied at the macrolevel. Various medical applications have always been a priority in the development of tomography, and the first tomographic studies of soils were performed with the use of medical tomographic equipment. Most of the works in the 1980s–1990s were performed on Siemens medical tomographs or their analogues [5, 6, 13, 69]. The equipment predetermined the shape of analyzed samples: cylindrical cores of undisturbed soil of various heights. These cores were relatively large—10–20 cm in diameter—and scanning resolution was about 100 μm and coarser.

However, the development of tomographic methods was not limited to medicine. Soon, it became clear that the tomograph is a good device for controlling the quality of industrial products for the presence of hidden defects. Powerful engineering devices—flaw detectors for industries and analyzers of geological cores similar in the size of the analyzed samples and in the power of the X-ray source—began to appear. Devices for studying the structure at the microlevel were just being developed, as was the software for them. Ten years have passed since the launch of the first X-ray tomograph until the publication of one of the first known works on soil tomography.

In 1982, the work [69] was published, where the authors determined the soil density using tomographic data. To assess the size of the pores, a plate with holes of different diameters (as a reference size standard) was used and scanned on a tomograph together with the sample. This method, despite imperfect equipment, made it possible to obtain data of better quality than SEM (scanning electron microscopy) data. At the same time, in the 1980s, it was suggested that SEM and tomography should be used together as complementary methods [88].

To a certain extent, the idea of computed tomography was ahead of its time. Tomography appeared almost 15 years before the mass distribution of IBM personal computers and the rapid development of computer processor technologies that simplified the work with tomographic data. The ability to digitize the internal volumetric structure of studied objects with subsequent division into X-ray contrast phases (for example, soil, pore space, mineral inclusions or nodules, and organic matter) is the basis for studying any volumetric structure as a physical object using a non-destructive method. However, the reconstruction of tomographic slices from shadow projections (the result of tomographic scanning) is a process that requires high-performance computer equipment. Note that this only the first stage, and segmentation (dividing an object into X-ray contrast phases according to shades of gray) and calculations of volumetric indicators are also demanding on computer technology and disk storage. As a result, at these stages, huge volumes of data are obtained, the possibilities of working with which are limited even at the modern level of the development of computer technology.

The unavailability (high cost, low prevalence) of computing power for reconstruction of tomographic slices, phase segmentation, and volumetric calculations was a serious problem at the early stages of tomography development. On the equipment of the 1980s (Iskra-226 computer), reconstruction of one slice took up to 7 min [88]. At the same time, there were problems with storing, processing, and outputting data.

To calculate the volumetric indicators used today, specialized software is used, which is not always available to researchers in our time, and which simply did not exist in the 1980s. An alternative to volume in terms of processing and calculation speed was the analysis of individual slices and further work with a set of statistical data. That is what is now called 2D image analysis.

At present, soil macrotomography is widely applied for a variety of tasks [9, 13, 59].

2D analysis of tomographic slices and the idea of cluster analysis. Digital image analysis even predates tomography. The first automatic segmentation algorithms were developed in the 1970s [67] and they are still used to work with tomographic data, although their use in soil tomography does not always guarantee an accurate result [4]. Initially, 2D analysis was used to work with SEM images. From there, the generally accepted characteristics were transferred to tomography: porosity, pore size distribution, average size, area, perimeter, and shape factor of a pore; structure anisotropy; etc. [88].

In the same time, the concept of tomographic porosity—porosity limited by the resolution of tomographic imaging—was developed.

Studies of soil microstructure necessitate not only qualitative but also quantitative characteristics of research objects. One of the most efficient methods is the distribution of pores in vertical sections of the soil based on the indicators of their orientation and shape. Some variants of cluster analysis of the characteristics of soil pores developed for thin sections [85] also found their application in the analysis of tomographic data [2]. For quantification, the *shape factor* was often used, sometimes in combination with pore orientation. Pore shape factor allows one to quantify the pore space of soils at different hierarchical levels. There are many options for evaluating the pore shape in 2D. The following variants are used most often:

(a) Shape factor (form factor *F*) proposed by Skvortsova [1] for the analysis of scanned images of thin sections. This indicator has certain advantages in characterizing the shape of pores in thin sections or tomographic sections and makes it possible to distinguish between several groups of macropores: from elongated fissures to rounded voids. In a number of publications [1, 82], this method is used in combination with cluster analysis [85]. It was also used to validate the quality of stochastic soil reconstructions [49]. Recently, an improvement was proposed to the Skvortsova classification, which makes it possible to distinguish between all types of pores by adding a convexity parameter to the equation [62].

(b) Other forms of the pore shape factor, e.g., the form factor (*FF*) used in the CT-an program (Bruker's proprietary software for processing tomographic data), which was originally made as a universal instrument for contrasting objects, but also proved to be useful for soil studies [13].

Analysis of soil pores in 2D sections has significant methodological limitations and is insufficient for studying anisometric pore space [1]. Thus, diametrically opposite results can be obtained for horizontal and vertical sections of the soil. Obviously, the Skvortsova shape factor can be extended for the analysis of 3D images of soils, although no such attempts have been made so far.

MODERN STAGE OF THE DEVELOPMENT OF CT (2000–PRESENT TIME). OVERALL TRANSITION TO ANALYSIS OF 3D STRUCTURES IN SOIL

Development and capabilities of modern tomographic equipment. At the end of the 1990s, the mass production of light-sensitive charge-coupled device (CCD) sensors (analog integrated circuits consisting of linked photosensitive photodiodes) of high resolution began. They were used in digital photography, but also influenced the development of tomography. On their basis, high-sensitive X-ray cameras were produced and found their application in tomography. This led to the appearance of inexpensive microtomographs, such as the SkyScan 1072 and 1074 models, the resolution of which was 5–10 times more detailed than that of medical equipment, but the size of the sample was greatly reduced (down to 1–3 cm in cross section). In the tomographs of these models, it was physically impossible to put a larger sample. Models of tomographs from General Electric retained the possibility of installing large samples, but at the same time the radiation source there in most cases was not powerful enough to penetrate a soil sample with a diameter larger than 6–7 cm. The design of a fourth-generation microtomograph dictates the rule: the smaller the sample, the more detailed the scanning resolution. This is true up to the resolution limit, which is about 60 nm in modern tomographs like the Bruker Skyscan 2214. Unfortunately, it is impossible to scan a soil core of 10 cm in diameter with a resolution of 60 nm on a tomograph, but a separate aggregate of 0.5–1 mm in size allows the transition to a submicron scale, which makes it possible to assess changes in the microstructure of soils under the impact of the long-term use of mineral fertilizers. It is technologically possible to design a tomograph that scans large samples with nano-resolution, but this will lead to the same problem that arose 30–40 years ago: a gigantic amount of data in shadow projections (hundreds of terabytes of information) [31], which can only be processed by a system such as a supercomputer or a large corporate server specially configured to solve such problems.

The development of indicators that assess the functional state of soils can be attributed to the modern tasks of tomography in soil science. This requires the study of the structure and microstructure of the solid phase and pore space of soils, the development of already existing indicators (e.g., the connectivity of the pores), and the development and testing of new mathematical and technical methods.

Microtomography and studies of soil structure and pore space of aggregates. The advent of new equipment also influenced soil tomography. It became possible to study the microstructure of aggregates of various soils with a fractional size of 250 μm and larger. In addition to the hardware, new software has also appeared. Bruker CTan has an object contouring mode with the ability to cut off internal pores (ROI shrink warp) that emerge on the sample surface at a specified threshold. This makes it possible to make a 3D analysis of the internal structure of the soil aggregate in 100% volume. The volumetric distribution of any structural elements of the X-ray contrast phases can be obtained.

At present, there is no alternative to computed tomography for studying the microstructure of aggregates. While aggregates of coarse fractions (7–10 mm and larger) can still be studied using traditional micro-

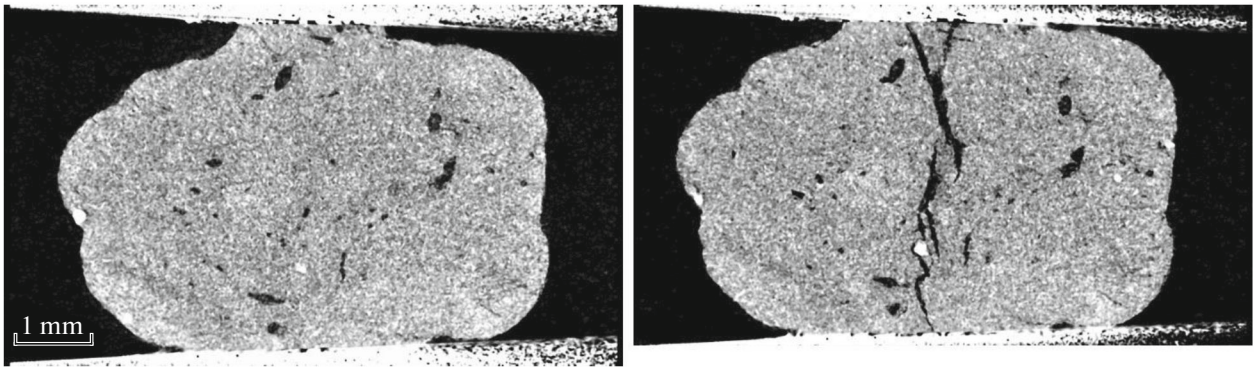

Fig. 1. Dry aggregate from a soddy-podzolic soil (Albic Retisol) before the load (left) and at the load of 600 g (right). CT scanning by K.A. Romanenko.

morphological methods, it is simply impossible to make thin sections from smaller aggregates. The thickness of a thin section is uneven; with good manual work, it is about 30 microns. With a scanning resolution of 3 μm, this corresponds to 10–11 tomographic sections forming their own volume, in which there will almost certainly be closed micropores. Owing to the contouring and high resolution, the results of tomographic scanning of a thin section can be combined with high accuracy (1–2 μm) manually, which will allow, in addition to morphometric parameters based on the analysis of tomographic data, to obtain data on the mineral composition based on the analysis of the thin section (or polished section).

There are not so many tomographic studies of the microstructure of aggregates as there are studies of soil at the macro level, but they are there, and there are some unusual and interesting works among them. Thus, using microtomography of chernozem aggregates, additional diagnostic criteria of negative processes of soil alkalization were provided: low values of the open porosity visible on tomographic images and the virtual absence of humus–clay plasma in the intraped zone [94]. In addition, microtomography has been applied to study the rate of decomposition of organic matter and its relationship with open pores [53]. The experience of morphological description inside the intraped pore space has also been published [87].

The results of mechanical load on soil aggregates can also be studied by microtomography. Computed tomography allows one to visualize the ongoing changes in the soil microstructure and record the load, at which such changes take place. The load on the aggregate is made in a special loading device for the tomograph. Also, when using such a device, load–deformation graphs can be analyzed. Such graphs show the peak load at which cracks appear in the aggregate (Fig. 1).

Pore space and segmentation of pores according to their genesis. The pore space of soils is a complex dynamic structure consisting of pores of various origins and shapes. Segmentation of the volumetric structure of the pore space is actually a visualization of the total porosity of the object under study. The dynamics of the total porosity in samples of any volume can be used as a diagnostic indicator [9], but, taken separately, it is of little interest. To assess the qualitative state of soils and their functions, indicators of the connectivity of the pore space, filtration models for water or air, and pore size distribution in the volumetric structure are much more informative. All this can be done on the basis of the already developed software (Image-J, ParaView, Avizo, etc.). However, if we do not take into account the organic matter in the soil, all these models will not work. Until recently, even if the roots in the pore-channels were clearly visible, it was practically impossible to separate the pores of phytogenic origin from other pores. Visualization of the volumetric structure of the pore space shows how different characteristic pores or types of pores form the general architecture of the pore space of the soil [68] and constitute a hierarchy of pores of different sizes and origins [22, 23]. The pores can be subdivided into textural pores determined by the arrangement of primary soil particles and larger structural pores. The latter are mainly formed by biological activity and tillage. The problem of analyzing the resulting complex structure is that pores of various sizes, shapes, and origins are repeatedly interconnected and cannot be divided into categories using existing indicators. There are currently two promising approaches to solving this problem:

(1) Identification and segmentation of structural pores according to their characteristic shape. This differentiation makes it possible to associate the pores with the processes of their formation. Thus, it has been shown that structural pores of phytogenic origin often form a dense network of cylindrical pores (biopores) [56, 58, 107]. Also, it is known that different methods of soil cultivation lead to the formation of pores of a characteristic shape [71, 72].

(2) Using a hierarchical sampling scheme and combining information on CT images from samples of

different sizes (soil samples of different sizes) and resolution to obtain a complete description of multiscale heterogeneity [7, 19, 29, 47, 91, 103]. By combining the pore size distribution (PSD) data on several sample sizes [102], it is possible to create a joint pore size distribution, which increases the size range of visible porosity.

A number of studies have found that biopores are fairly well isolated from pores of other origins. This allows them to be segmented with high reliability and separated from the rest of the pore space. The authors of [107] presented their own method of biopore segmentation.

Study of soil structure and soil pore space using correlation functions. The theory of local porosity [11], pore size distribution, tortuosity, and other parameters [57] can be used to quantitatively characterize the three-dimensional structure of the soil as a geophysical medium and its connectivity. However, all these useful characteristics only describe different aspects of the structure of the porous medium, a universal descriptor (this term should be understood as a quantitative indicator reflecting all the necessary features) of the pore space and soil structure does not exist at the moment. To describe the structure of an object, ideally, it must be mathematically represented in the form of some function or a set of parameters of such a function. In addition to the existence of such a formulation of the problem, it is also necessary to solve the opposite problem, i.e., to restore the structure from its function, which is usually called reconstruction [45, 98].

The verification of the possibility of describing and restoring the pore space and soil structure from two-point correlation functions by the simulated annealing (SA) method is presented by the authors of the corresponding article [30]. It should be noted that this article was written on the basis of the results of the analysis of 2D images (scanned thin sections), but it can also be applied to tomographic sections.

According to the results of the study, out of the eight types of soil pore space, the same type of pore distribution in shape and orientation in the original and reconstructed images was observed only in two cases. The most successful reconstruction based on the morphometric parameters of the pores was obtained for a massive soil structure with scattered rounded pores. It was found that problems with reconstruction arise due to a large number of differently oriented fissures. Thus, though the method of mathematical reconstruction of the pore space of the soil at the current stage is far from being perfect, it can be successfully used for soils and rocks with isometric (in 2D sections) pores. Isometric pores are characteristic of the massive structure of loamy soil-forming rocks with rounded biogenic pores and for crumb structure of humus horizons with isometric dissected packing voids of crumb aggregates. To improve the description of soil structure and pore space with the use of correlation functions, studies in three directions seem to be promising: (1) combined use of other types of functions (cluster, linear, chord, etc.), (2) development of a method to take soil anisotropy into account, and (3) use of multipoint correlation functions [30].

In 2015, a universal stochastic method for combining multiscale images based on scalable correlation functions was developed while working on the reconstruction with the use of correlation functions and optimization by the simulated annealing method. The new method can potentially be used for various scientific and applied purposes, including obtaining images with the so-called super resolution (a resolution higher than that provided by the device) [27]. A team of authors solved the problem of comparing two soil structures on the basis of correlation functions by analyzing the contribution of each correlation function to the optimization function when solving the inverse problem of stochastic reconstruction [27]. Based on the comparison of the structures, it is possible to estimate the statistical homogeneity of the structure of soil pore space [33, 34], which is directly related to the representativeness of the soil structure and various physical properties in the studied volume, up to the classical undisturbed samples. According to the parametrization of correlation functions, it is possible to compress information about the structure of soils and build a digital model of a 3D structure of any hierarchy and complexity [48].

MORPHOMETRIC INDICATORS IN THE ANALYSIS OF VOLUMETRIC STRUCTURES AT DIFFERENT LEVELS OF THE STRUCTURAL ORGANIZATION OF SOILS

With the advent of 3D analysis of tomographic data, it became necessary to develop volumetric indicators for assessing the state of soils. Initially, some of the indicators were borrowed from 2D analysis (image analysis)—total porosity and the number of objects (pores)—and adapted for 3D structures. However, the volumetric structure is very different from the 2D image. In the volume, the pores are connected, and a situation may arise when the total porosity of the soil according to tomographic data is more than 50% in a volume of 1 cm^3, whereas there is only one pore in this volume [94].

Over time, indicators of open and closed porosity were developed and included in programs for analyzing tomographic data (for example, CTan), where *closed porosity* is the fraction of the total volume of isolated pores in the sample volume, and *open porosity* is the fraction of the total pore volume reaching the surface [18]. These parameters are useless without reference to volume, because the larger the volume, the larger the closed porosity. At the same time, it is quite acceptable to use them for objects of comparable sizes, e.g., for soil aggregates of the same fractional size.

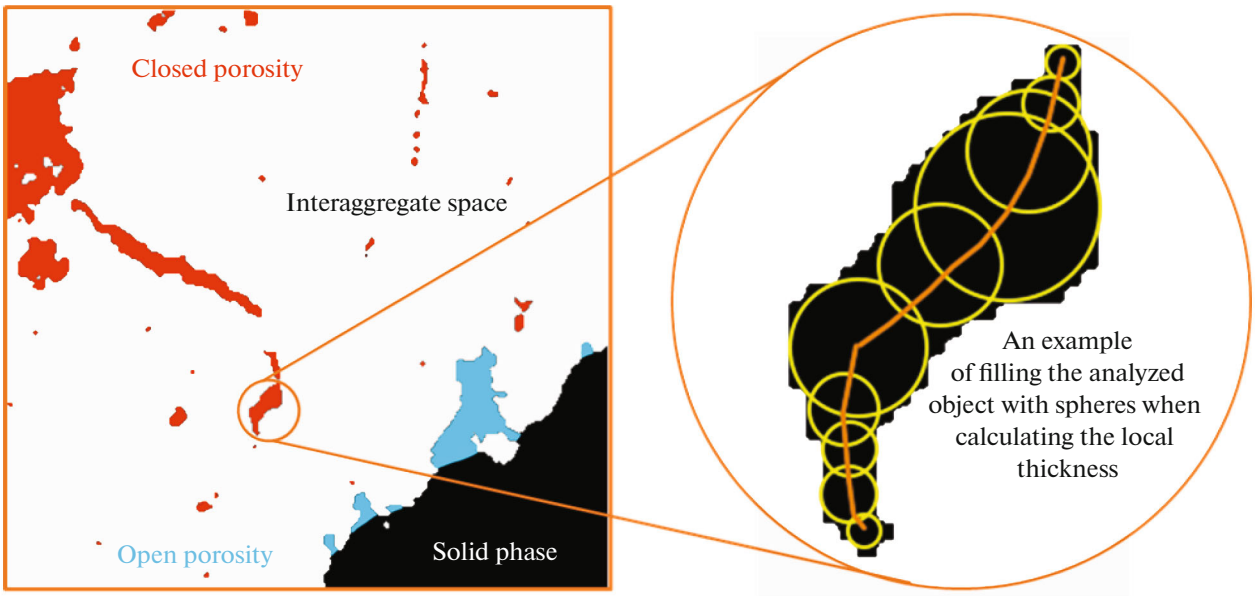

Fig. 2. Calculation of the local thickness of scanned object in 2D (according to [106]).

With the development of 3D analysis, the concept of the local thickness of an object was formed [15]. *Local thickness* is an estimated parameter, programmatically determined by filling the internal structure of an object with spheres. The method for calculating the local pore thickness in 2D is shown in Fig. 2; in 3D, the program analyzes the most distant from one another points of the pore, and builds a "skeletal" line between them through the geometric center of the pore; then, it begins to fill the internal volume with spheres, where the center of the sphere is located on the skeletal line, and the edge is the nearest border of the pore.

As a result, a map of the local pore space thickness is formed, where the pore space volume is divided into size fractions (the proportion of the volume occupied by spheres of a certain size fraction). In a sense, this indicator is more informative than the usual "average pore radius." If the fractured pore in the cross section is a broken line, then it is a plane similar to a crumpled sheet of paper of different thickness in the volume. If it partially goes beyond the resolution, then it is a sheet with holes. In this case, the average radius will be low-informative, and the local thickness will show the pore thickness and the distribution of volumes relative to the thickness. It becomes possible to construct a volumetric map of the local thickness of any X-ray contrast phase, such as germinated seed, mineral grains, or the structure of the pore space inside the aggregate with a very high resolution (Fig. 3).

Local thickness as an estimated quantitative indicator is still rare in research; it is known to be used for calculating the pore space of gray forest soil (Greyzemic Phaeozem Albic) [84, 104] and aggregates [106].

The method of numerical analysis of three-dimensional tomographic images based on integral geometry, topology, and morphological analysis was tested on soil samples. This method implies the calculation of the cumulative and noncumulative distributions of pores in terms of the sizes of the Minkowski functions and Betti numbers [43, 103].

The quantitative indicators have also undergone changes. If it is possible to determine the closed porosity, then *the number of closed pores* can be calculated. Knowing the threshold of water permeability and *the local thickness* of the pore space at a given resolution, it is possible to estimate the functional role of pores, for example, in filtration or water retention. One of the urgent problems in the analysis of the volumetric structure of the pore space is the assessment of the pore connectivity.

The connected volumetric structure of the pore space can be estimated in terms of connectivity parameters. *The connectivity of the pore space* is an important parameter that determines the integrity and intactness of the pore space structure [77]. Connectivity can be the basis for determining air permeability and saturated hydraulic conductivity [59, 107]. Moreover, the relationship between different classes of pores is also important for soil as a habitat for many organisms, as well as for the availability of soil organic carbon (SOC) for these organisms and their state of aeration [53, 64].

One of the most commonly used pore connectivity metrics is the Euler number. Euler's number measures what might be called "excess connectivity"—the degree to which parts of an object are repeatedly connected [65]. It is a measure of how many connections

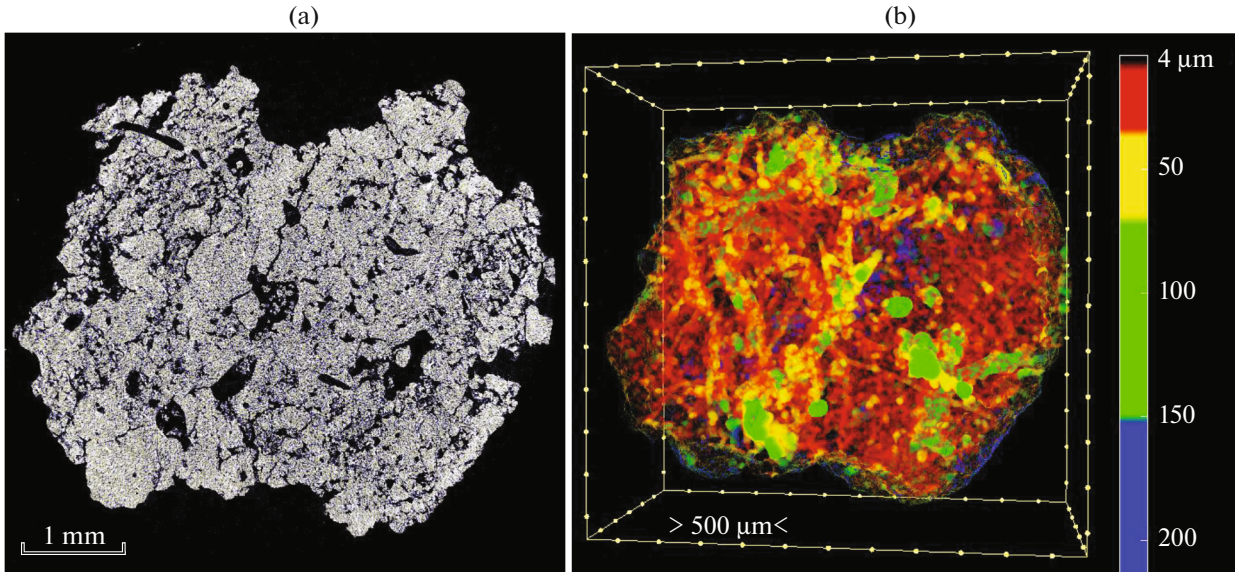

Fig. 3. Modeling the pore space of a typical chernozem aggregate: (a) a tomographic section through the center of the sample (pores are black); (b) the result of processing and calculation of the local pore thickness in the aggregate volume (from the resolution limit to the maximum thickness of the object). The soil sample was provided by V.A. Kholodov. Scanning, processing, and modeling were carried out by K.N. Abrosimov.

in a structure can be broken before it splits into two separate pieces. (Topologically, an object can be compressed into a circle, and redundant joints look like "handles".) The components of the Euler number are three Betti numbers: β_0 is the number of unconnected objects (clusters), β_1 is the number of redundant joints, and β_2 is the number of closed cavities. The Euler-Poincaré formula for a three-dimensional object X is given:

$$\chi(X) = \beta_0 - \beta_1 + \beta_2.$$

When calculating the Euler number of an individual object, β_0 is always equal to unity. The values of β_1 and β_2 will determine the Euler number of an individual object [101]. The number of closed cavities in the soil is usually insignificant [102]. If we neglect β_2, χ becomes negative, if the number of redundant connections exceeds the number of unconnected clusters, and positive, if vice versa. For a pore space with many connections, the Euler number will be negative, and for a pore space with many isolated pores, it will be positive.

The χ number is a global metric that can be efficiently calculated from the frequency of local pixel configurations within $2 \times 2 \times 2$ voxel neighborhoods. It is independent of the size of the connected clusters. Thus, negative χ does not necessarily mean that there is a long-distance connection through the associated pore cluster [80, 102].

In addition to the Euler number, a dimensionless Γ-*indicator* has been developed that is sensitive to long-distance coupling, that is, its value is higher, if most of the porosity belongs to the largest linked cluster [58, 80]:

$$\Gamma_p = \frac{1}{N_p^2}\sum_{k=1}^{N_i} n_k^2,$$

where N_p is the number of all pore voxels p, N_i is the number of all clusters, and n_k is the number of pore voxels in cluster k. Γ reflects the probability that two randomly selected pore voxels belong to the same pore cluster and are strongly influenced by the largest pore cluster n_k [44]. It can range from 0 (many unconnected clusters) to 1, when all pore voxels belong to the same linked cluster. Γ-indicator usually increases with increasing porosity along an *s*-shaped curve without a clear percolation threshold [80]. The slope of this curve reflects the change in the size of the associated pore clusters, i.e., it is a measure of the variability of percolation between samples of the dataset [80]. Thus, Γ-indicator reflects the probability of detecting a continuous path through the pore system, and χ reflects the number of internal connections without taking into account their length [40].

In the works of the last 20 years, the Euler number is almost always encountered, when the pore space of the soil is determined as the object of study, and the connectivity of the pore space is chosen as the criterion for assessing its state [7, 43, 53, 64]. Recent developments in the field of describing the structure of porous media suggest that the Minkowski functionals can be successfully unified with correlation functions, since they are a subset of them [60, 61].

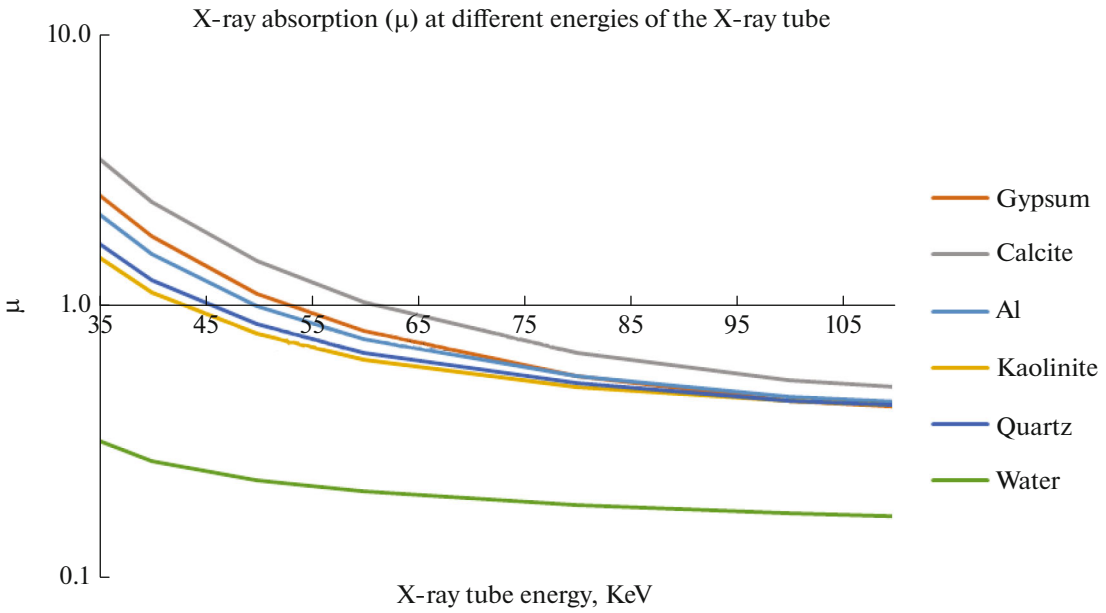

Fig. 4. Brightness distribution of elements in dependence on the absorption coefficient against the background of water sorption. The graph is based in the MuCalcTool database for minerals and rocks.

PROSPECTS OF COMUTED TOMOGRAPHY IN SOIL STUDIES

Dual energy method and its application for soil objects. Dual energy computed tomography (DECT) implies scanning of the same sample at two different energies of the X-ray source. For example, at 40 and 100 KeV. In DECT, several X-ray spectra are used to characterize the attenuation of photons depending on the material. Processing of such data allows one to see what is not visible at any one energy of the source.

The fact is that the number of X-ray contrast phases that we observe depends on the change in the scanning energy. There are many clay minerals in the soil, the X-ray absorption of which coincides in most cases, so that they are represented by the same shade of gray on tomographic sections, but there are also differences (Fig. 4). For example, at the energy of 40 keV, most of the clay minerals and elements present on the graph will be distinguishable from each other and will be represented by their own grade of gray. At the energy of 100 keV, only the pore space with water and calcite will remain distinguishable. The rest of the elements will merge into one shade of gray.

Leaving only one (lower) energy level is not always the right decision. There are minerals that can change their places on the graph at different energies; the grades of gray at 40 and 100 keV will actually remain the same, but they will correspond to different elements. Knowing this fact, we can choose the energy, at which the grades of gray for these minerals will be indistinguishable as background data. Further, after processing the data stacks, it will be possible to judge the distribution of each of the elements in the sample with high accuracy.

In medicine, the dual energy method is considered new and revolutionary [96]. In soil science, it is rarely used, though it is known for a long time. Thus, this method can be used to calculate soil density and water content [12, 17]. Potentially, this method can allow solving the inverse problem and reconstruct the amount of phase in each voxel [100, 105]. However, the use of such technologies for the analysis of soils can be difficult because of the significant chemical heterogeneity of soils. The dual energy method opens up possibilities for developing contrasting of X-ray contrast phases that are weakly visible at certain energies.

Combination of FIB–SEM data and computed tomography. The combination of computed tomography and electron microscopy methods is a promising direction. Considering the small size of the study object, the tomographic data at the resolution limit can be combined with the results of the scanning electron microscopy with ion beam columns (FIB–SEM). Such a study was carried out in 2020: computed tomography data were combined with FIB–SEM data for an area of 50 μm^2 [31]. The tomographic data resolution was 1 μm, and the FIB–SEM resolution was up to 2.5 nm.

The data obtained can be useful for characterizing the pore size distribution, in the range from 2.5 nm to ~ 1 μm. Three main types of nanoporosity have been described: (a) between mineral grains and organomineral complexes, (b) within the organic matter, and (c) in the minerals. At present, this method has a number of serious drawbacks: very small size (volume) of the studied object and, hence, low represen-

tativeness; lack of methods for processing FIB–SEM images, especially for pore segmentation; high cost; damage arising from milling a sample for FIB–SEM; effects of cryogenic processing; etc.

However, obvious advantages of this approach are the detailing of pores and differentiation of materials via local probing of the chemical composition and possibility to apply numerical modeling for nanoscale processes (flows, microbial activity, etc.) [31].

Possibilities of neural networks in the processing and analysis of tomographic data. A significant difficulty inherent in any method of image analysis (tomographic slice, photograph of a thin section, SEM image, etc.) is the need to select threshold values for separating the materials composing sample, or the so-called segmentation. As we noted above, pixels/voxels at phase boundaries often contain several materials. Many complex methods and automatic algorithms have been developed for image segmentation [66, 67, 89], but the diversity of methods has no positive effect on their efficiency.

In recent years, neural network technologies have found wide application in the field of image processing. Modern approaches to local segmentation can provide reliable data for training a neural network of tomographic image segmentation. In the study [54], the authors used the hybrid architecture U-net + ResNet-101; 7 tomographic images of the soil were applied for test segmentation. Training was performed by excluding the segmented image from the training and validation datasets. The segmentation accuracy was assessed using standard computer vision metrics (accuracy, sensitivity, intersection over union (IoU), etc.) and pore-scale simulation to calculate the permeability of the resulting 3D binary soil images. Depending on the soil sample, the segmentation error according to the calculated hydraulic properties varied from 5 to 130%. Although the synthetic tomography method is still not developed enough to provide us with reliable data modeled with the necessary physical realism, the methodology proposed in this article is already applicable to solving a number of practical problems:

(1) Having a large set of training data from tomographic images, it is possible to build a convolutional neural network (CNN) that will segment computed tomography data of soils much faster and without an operator than the already known methods, such as kriging or convergence of active contours, which require large computational costs.

(2) The CNN methodology can be trained to segment FIB–SEM images of soil structure at the nanoscale [31], where traditional segmentation methods for tomographic images are not applicable [54].

Possibilities of open-source codes and software for modeling the physical properties of soil on the basis of data on its structure. Once the 3D images are separated into phases, in the simplest case, pores and solids, this information can be used to simulate physical properties, including hydraulic and transport characteristics. All such techniques can be roughly divided into two classes: direct models and simplified algorithms. The first, for example, include techniques for solving the Navier–Stokes equations for modeling one- and two-phase filtration of fluids in pores. The most popular direct methods are the (1) lattice Boltzmann method LBM [50, 75]; (2) finite element method FEM, finite volume method FVM and volume of fluid method VoF [78, 10]; (3) hydrodynamics of smoothed particles SPH method [41]; (4) finite difference method FDM applied for the Laplace and Stokes equations [32, 86]; (5) level set method [76]; and (6) phase-field or density functional method [20, 81]. However, all these computational methods require significant computational resources, which limits the size of the simulation region, in which computations can be performed to a very limited volume, usually up to ~ 700^3 voxels. However, computations for such seemingly very small domains, even using high-performance computing resources, may require several weeks with significant parallelization across hundreds of computational cores. These problems often preclude the ability to work with representative elementary volumes (REV) of soils, as well as with composite images. The only practical option is to use indirect modeling methods, such as pore-network models (PNM) [24–26], which in fact can be efficiently parameterized using direct pore scale modeling by any of the above methods [62, 79]. Although PNMs allow efficient computations to simulate one-, two-, and even three-phase filtration, in order to use them, it is first necessary to extract a porous network model from a 3D image [8, 34]. Currently, there is a set of open codes and free software for pore-network modeling, including the solution of the Stokes FDMSS equation [32] or the solution for non-Newtonian fluids [21], modules for OpenFOAM for direct modeling of one- and two-phase flows [78], libraries for the selection of porous network models PoreSpy and calculations in them OpenPNM [36–38]. At the same time, the extraction of the PNM from a 3D image allows us to conduct a more accurate analysis of the pore size distribution in comparison with the simple morphological methods described above.

CONCLUSIONS

Based on the analysis of publications on tomographic studies in the field of soil science, it is possible to determine the main directions ways of further development of computed tomography in soil science:

(1) Further development of the instrumental and analytical base will make it possible in the near future to obtain high-quality ultrahigh-resolution tomographic data;

(2) The development of segmentation based on self-learning neural networks; if successful, it will cre-

ate a service for smart data segmentation. This does not mean cancelling of manual segmentation and existing algorithms everywhere and at once, but will allow us to overcome one of the bottlenecks of soil CT, where the role of human factor is high; in the future, such a segmentation will serve as the basis for express analysis of soil structure based on tomographic data;

(3) The knowledge base on the structure and pore space of soils will be supplemented by new research from various regions of the world. Several years ago, the experience of multiscale soil studies was tested, and this was a step towards an integrated approach to the study of the entire soil profile, and possibly a step towards a mathematical description of the soil structure at the regional level with forecasting and risk assessment;

(4) Improvement of calculation methods. Already, there are many open source programs for data visualization and filters for tomographic images, which are in no way inferior in functionality to commercial models [54], but often without a friendly interface. The appearance of software packages partially or completely made for the analysis of soil images, by analogy with the already existing SoilJ (plug-in for ImageJ) [52], including software for modeling fluid flow in the soil, can be expected.

FUNDING

This study was supported by the Russian Science Foundation, project no. 19-74-10070; the equipment of the Center for Collective Use "Functions and Properties of Soils and Soil Cover" at the V.V. Dokuchaev Soil Science Institute (registration number 441994, https://ckp-rf.ru/ckp/441994/) was used.

CONFLICT OF INTEREST

The authors declare that they have no conflicts of interest.

REFERENCES

1. E. B. Skvortsova, K. M. Gerke, D. V. Korost, and K. N. Abrosimov, "The pore space arrangement in podzolic horizons of loamy soils (analysis of 2D and 3D images)," Byull. Pochv. Inst. im. V.V. Dokuchaeva, No. 71, 65–79 (2013).
2. E. B. Skvortsova and N. V. Kalinina, "Micromorphometric types of the pore space in virgin and plowed loamy soils," Eurasian Soil Sci. **37**, 980–991 (2004).
3. *Explanatory Dictionary of Soil Science*, Ed. by A. A. Rode (Nauka, Moscow, 1975) [in Russian].
4. K. N. Abrosimov, K. M. Gerke, I. N. Semenkov, and D. V. Korost, "Otsu's algorithm in the segmentation of pore space in soils based on tomographic data," Eurasian Soil Sci. **54**, 560–571 (2021).
5. S. H. Anderson and C. J. Gantzer, "Determination of soil water content by X-ray computed tomography and magnetic resonance imaging," Irrig. Sci. **10** (1), 63–71 (1989).
6. L. A. G. Aylmore and J. M. Hainsworth, "The use of computed assisted tomography to determine spatial distribution of soil water content," Aust. J. Soil Res. **21**, 435–443 (1983).
7. A. Bacq-Labreuil, J. Crawford, S. J Mooney, A. L. Neal, E. Akkari, C. McAuliffe, X. Zhang, M. Redmile-Gordon, and K. Ritz, "Effects of cropping systems upon the three-dimensional architecture of soil systems are modulated by texture," Geoderma **332**, 73–83 (2018). https://doi.org/10.1016/j.geoderma.2018.07.002
8. T. G. Baychev, A. P. Jivkov, A. Rabbani, A. Q. Raeini, Q. Xiong, T. Lowe, and P. J. Withers, "Reliability of algorithms interpreting topological and geometric properties of porous media for pore network modeling," Transp. Porous Media **128**, 271–301 (2019).
9. A. A. Belik, A. A. Kokoreva, A. G. Bolotov, A. V. Dembovetskii, V. N. Kolupaeva, D. V. Korost, and A. N. Khomyak, "Characterizing macropore structure of agrosoddy-podzolic soil using computed tomography," Open Agric. **5**, 888–897 (2020). https://doi.org/10.1515/opag-2020-0080
10. C. Bilger, M. Aboukhedr, K. Vogiatzaki, and R. S. Cant, "Evaluation of two-phase flow solvers using Level Set and Volume of Fluid methods," J. Comput. Phys. **345**, 665–686 (2017).
11. B. Biswal, C. Manwart, and R. Hilfer, "Three-dimensional local porosity analysis of porous media," Phys. A (Amsterdam) **255**, 221–241 (1998).
12. D. Braz, R. T. Lopes, and L. M. G. Motta, "Dual-energy computerized tomography in compacted soil," Geotech. Geol. Eng. **18**, 221–238 (2000).
13. Y. Capowiez, A. Pierret, P. Monestiez, and L. Belzunces, "Evolution of burrow systems after the accidental introduction of a new earthworm species into a Swiss pre-alpine meadow," Biol. Fertil. Soils **31**, 494–500 (2000).
14. Y. Capowiez, S. Sammartino, and E. Michel, "Using X-ray tomography to quantify earthworm bioturbation non-destructively in repacked soil cores," Geoderma **162**, 124–131 (2011).
15. M. Y. M. Chiang, F. A. Landis, X. Wang, J. R. Smith, M. T. Cicerone, J. Dunkers, and Y. Luo, "Local thickness and anisotropy approaches to characterize pore size distribution of three-dimensional porous networks," Tissue Eng., Part C **15**, 65–76 (2009). https://doi.org/10.1089/ten.tec.2008.0298
16. A. Cormack, "Representation of a function by its line integrals, with some radiological applications," J. Appl. Phys. **34** (9), 2722–2727 (1963).
17. S. Crestana, PhD Thesis (Säo Paulo, 1985).
18. *CTan Usermanual: Morphometric Parameters Measured by Skyscan™ CT-Analyser Software* (Bruker, Billerica, MA, 2013).
19. N. Dal Ferro, L. Sartori, G. Simonetti, A. Berti, and F. Morari, "Soil macro- and microstructure as affected by different tillage systems and their effects on maize root growth," Soil Tillage Res. **140**, 55–65 (2014). https://doi.org/10.1016/j.still.2014.02.003

20. A. Demianov, O. Dinariev, and N. Evseev, "Density functional modeling in multiphase compositional hydrodynamics," Can. J. Chem. Eng. **89** (2), 206–226 (2011).
21. P. Eichheimer, M. Thielmann, A. Popov, G. J. Golabek, W. Fujita, M. O. Kottwitz, and B. J. P. Kaus, "Pore-scale permeability prediction for Newtonian and non-Newtonian fluids," Solid Earth **10** (5), 1717–1731 (2019).
22. T. R. Elliot and R. J. Heck, "A comparison of optical and X-ray CT technique for void analysis in soil thin section," Geoderma **141**, 60–70 (2007).
23. E. T. Elliott and D. C. Coleman, "Let the soil work for us," Ecol. Bull. **39**, 23–32 (1998).
24. I. Fatt, "The network model of porous media I. Capillary pressure," Trans. AIME **207**, 144–159 (1956).
25. I. Fatt, "The network model of porous media II. Dynamic properties of a single size tube network," Trans. AIME **207**, 160–163 (1956).
26. I. Fatt, "The network model of porous media III. Dynamic properties of networks with tube radius distribution," Trans. AIME **207**, 164–181 (1956).
27. K. M. Gerke and M. V. Karsanina, "Improving stochastic reconstructions by weighing correlation functions in an objective function," Europhys. Lett. **111** (5), 56002 (2015). https://doi.org/10.1209/0295-5075/111/56002
28. K. M. Gerke and M. V. Karsanina, "How pore structure non-stationarity compromises flow properties representativity (REV) for soil samples: pore-scale modelling and stationarity analysis," Eur. J. Soil Sci., (2020). https://doi.org/10.1111/ejss.13055
29. K. M. Gerke, M. V. Karsanina, and D. Mallants, "Universal stochastic multiscale image fusion: an example application for shale rock," Sci. Rep. **5**, 15880 (2015). https://doi.org/10.1038/srep15880
30. K. M. Gerke, M. V. Karsanina, and E. V. Skvortsova, "Description and reconstruction of the soil pore space using correlation functions," Eurasian Soil Sci. **45**, 861–872 (2012). https://doi.org/10.1134/S1064229312090049
31. K. M. Gerke, E. V. Korostilev, K. A. Romanenko, and M. V. Karsanina, "Going submicron in the precise analysis of soil structure: a FIB-SEM imaging study at nanoscale," Geoderma **383**, 114739 (2021). https://doi.org/10.1016/j.geoderma.2020.114739
32. K. M. Gerke, E. B. Skvortsova, and D. V. Korost, "Tomographic method of studying soil pore space: current perspectives and results for some Russian soils," Eurasian Soil Sci. **45**, 700–709 (2012).
33. K. M. Gerke, T. O. Sizonenko, M. V. Karsanina, E. V. Lavrukhin, V. V. Abashkin, and D. V. Korost, "Improving watershed-based pore-network extraction method using maximum inscribed ball pore-body positioning," Adv. Water Res. **140**, 103576 (2020).
34. K. M. Gerke, R. V. Vasilyev, S. Khirevich, D. Collins, M. V. Karsanina, T. O. Sizonenko, D. V. Korost, S. Lamontagne, and D. Mallants, "Finite-difference method Stokes solver (FDMSS) for 3D pore geometries: software development, validation and case studies," Comput. Geosci. **114**, 41–58 (2018). https://doi.org/10.1016/j.cageo.2018.01.005
35. S. N. Gorbov, O. S. Bezuglova, K. N. Abrosimov, E. B. Skvortsova, S. S. Tagiverdiev, and I. V. Morozov, "Physical properties of soils in Rostov agglomeration," Eurasian Soil Sci. **49**, 898–907 (2016).
36. J. T. Gostick, Z. A. Khan, T. G. Tranter, M. D.R. Kok, M. Agnaou, M. Sadeghi, and R. Jervis, "PoreSpy: A python toolkit for quantitative analysis of porous media images," J. Open Source Software **4** (37), 1296 (2019).
37. J. T. Gostick, "Versatile and efficient pore network extraction method using marker-based watershed segmentation," Phys. Rev. E **96** (2), (2017).
38. J. Gostick, M. Aghighi, J. Hinebaugh, T. Tranter, M. A. Hoeh, H. Day, B. Spellacy, M. H. Sharqawy, A. Bazylak, A. Burns, and W. Lehnert, "OpenPNM: a pore network modeling package," Comput. Sci. Eng. **18** (4), 60–74 (2016).
39. Z. He, S. Zhang, J. Teng, Y. Yao, and D. Sheng, "A coupled model for liquid water-vapor-heat migration in freezing soils," Cold Reg. Sci. Technol. **148**, 22–28 (2018). https://doi.org/10.1016/j.coldregions.2018.01.003
40. A. L. Herring, L. Andersson, S. Schlüter, A. Sheppard, and D. Wildenschild, "Efficiently engineering pore-scale processes: the role of force dominance and topology during nonwetting phase trapping in porous media," Adv. Water Res. **79**, 91–102 (2015). https://doi.org/10.1016/j.advwatres.2015.02.005
41. D. W. Holmes, J. R. Williams, P. Tilke, and C. R. Leonardi, "Characterizing flow in oil reservoir rock using SPH: absolute permeability," Comput. Part. Mech. **3**, 141–154 (2016). https://doi.org/10.1007/s40571-015-0038-7
42. G. N. Hounsfield, "Computerized transverse axial scanning (tomography). Description to system," Br. J. Radiol. **46**, 1016–1022 (1973).
43. D. Ivonin, T. Kalnin, E. Grachev, and E. Shein, "Quantitative analysis of pore space structure in dry and wet soil by integral geometry methods," Geosciences **10** (9), 365–365 (2020).
44. N. Jarvis, M. Larsboand, and J. Koestel, "Connectivity and percolation of structural pore networks in a cultivated silt loam soil quantified by X-ray tomography," Geoderma **287**, 71–79 (2017). https://doi.org/10.1016/j.geoderma.2016.06.026
45. Y. Jiao, F. H. Stillinger, and S. Torquato, "Modeling heterogeneous materials via two-point correlation functions: basic principles," Phys. Rev. **76**, 031110 (2007).
46. M. Joschko, O. Graff, P. C. Müller, K. Kotzke, P. Lindner, D. P. Pretschner, and O. Larink, "A nondestructive method for the morphological assessment of earthworm burrow systems in three dimensions by X-ray computed tomography," Biol. Fertil. Soils **11**, 88–92 (1991).
47. M. V. Karsanina, K. M. Gerke, E. V. Skvortsova, A. L. Ivanov, and D. Mallants, "Enhancing image resolution of soils by stochastic multiscale image fusion," Geoderma **314**, 138–145 (2018). https://doi.org/10.1016/j.geoderma.2017.10.055

48. M. V. Karsanina, K. M. Gerke, E. V. Skvortsova, and D. Mallants, "Universal spatial correlation functions for describing and reconstructing soil microstructure," PLoS One **10** (5), e0126515 (2015).
49. M. V. Karsanina, E. V. Lavrukhin, D. S. Fomin, A. V. Yudina, K. N. Abrosimov, and K. M. Gerke, "Compressing soil structural information into parameterized correlation functions," Eur. J. Soil Sci., (2020). https://doi.org/10.1111/ejss.13025
50. S. Khirevich, I. Ginzburg, and U. Tallarek, "Coarse- and fine-grid numerical behavior of MRT/TRT lattice-Boltzmann schemes in regular and random sphere packings," J. Comput. Phys. **281**, 708–742 (2015).
51. N. Koebernick, K. R. Daly, S. D. Keyes, T. S. George, L. K. Brown, A. Raffan, L. J. Cooper, M. Naveed, A. G. Bengough, I. Sinclair, P. D. Hallett, and T. Roose, "High-resolution synchrotron imaging shows that root hairs influence rhizosphere soil structure formation," New Phytol. **216** (1), 124–135 (2017). https://doi.org/10.1111/nph.14705
52. J. Koestel, "SoilJ: an ImageJ plug-in for the semiautomatic processing of three-dimensional X-ray images of soils," Vadose Zone J. **17** (1), 170062 (2018).
53. A. N. Kravchenko, W. C. Negassa, A. K. Guber, and M. L. Rivers, "Protection of soil carbon within macroaggregates depends on intra-aggregate pore characteristics," Sci. Rep. **5**, 291 (2015). https://doi.org/10.1038/srep16261
54. E. V. Lavrukhin, K. M. Gerke, K. A. Romanenko, K. N. Abrosimov, and M. V. Karsanina, "Assessing the fidelity of neural network-based segmentation of soil XCT images based on pore-scale modelling of saturated flow properties," Soil Tillage Res. **209** (15), 104942 (2021). https://doi.org/10.1016/j.still.2021.104942
55. M. P. Lebedeva, D. L. Golovanov, V. A. Shishkov, A. L. Ivanov, and K. N. Abrosimov, "Microscopic and tomographic studies for interpreting the genesis of desert varnish and the vesicular horizon of desert soils in Mongolia and the USA," Bol. Soc. Geol. Mex. **71** (1), 21–42 (2019).
56. M. Leue, D. Uteau-Puschmann, S. Peth, J. Nellesen, R. Kodešová, and H. H. Gerke, "Separation of soil macropore types in three-dimensional x-ray computed tomography images based on pore geometry characteristics," Vadose Zone J. **18**, 1–13 (2019). https://doi.org/10.2136/vzj2018.09.0170
57. W. B. Lindquist, S.-M. Lee, D. A. Coker, K. W. Jones, and P. Spanne, "Medial axis analysis of void structure in three-dimensional tomographic images of porous media," J. Geophys. Res.: Solid Earth **101**, 8297–8310 (1996).
58. M. Lucas, S. Schlüter, H.-J. Vogel, and D. Vetterlein, "Soil structure formation along an agricultural chronosequence," Geoderma **350**, 61–72 (2019). https://doi.org/10.1016/j.geoderma.2019.04.041
59. L. Luo, H. Lin, and S. Li, "Quantification of 3-D soil macropore networks in different soil types and land uses using computed tomography," J. Hydrol. **39** (1–2), 53–64 (2010).
60. Z. Ma and S. Torquato, "Precise algorithms to compute surface correlation functions of two-phase heterogeneous media and their applications," Phys. Rev. E **98** (1), 013307 (2018).
61. Z. Ma and S. Torquato, "Generation and structural characterization of Debye random media," Phys. Rev. E **102** (4), 043310 (2020).
62. X. Miao, K. M. Gerke, and T. O. Sizonenko, "A new way to parameterize hydraulic conductances of pore elements: a step forward to create pore-networks without pore shape simplifications," Adv. Water Res. **105**, 162–172 (2017).
63. S. J. Mooney, T. P. Pridmore, J. Helliwell, and M. J. Bennett, "Developing X-ray computed tomography to non-invasively image 3D root systems architecture in soil," Plant Soil **352** (1–2), 1–22 (2012). https://doi.org/10.1007/s11104-011-1039-9
64. W. C. Negassa, A. K. Guber, A. N. Kravchenko, T. L. Marsh, B. Hildebrandt, and M. L. Rivers, "Properties of soil pore space regulate pathways of plant residue decomposition and community structure of associated bacteria," PLoS One **10**, e0123999 (2015). https://doi.org/10.1371/journal.pone.0123999
65. A. Odgaard and H. J. Gundersen, "Quantification of connectivity in cancellous bone, with special emphasis on 3-D reconstructions," Bone **14** (2), 173–182 (1993).
66. W. Oh and B. Lindquist, "Image thresholding by indicator kriging," IEEE Trans. Pattern Anal. Mach. Intell. **21**, 590–602 (1999).
67. N. Otsu, "A threshold selection method from gray-level histograms," IEEE Trans. Syst. Man Cybern. **9**, 62–66 (1979). https://doi.org/101109/TSMC19794310076
68. M. Pagliai and N. Vignozzi, "Soil pore system as an indicator of soil quality," Adv. GeoEcol. **35**, 71–82 (2002).
69. A. M. Petrovic, J. E. Siebert, and P. E. Rieke, "Soil bulk density analysis in three dimensions by computed tomographic scanning," Soil Sci. Soc. Am. J. **46** (3), 445–450 (1982). https://doi.org/10.2136/sssaj1982.03615995004600030001x
70. R. L. Peyton, B. A. Haeffner, S. H. Anderson, and C. J. Gantzer, "Applying X-ray CT to measure macropore diameters in undisturbed soil cores," Geoderma **53** (3–4), 329–340 (1992).
71. L. F. Pires, J. A.R. Borges, J. A. Rosa, M. Cooper, R. J. Heck, S. Passoni, and W. L. Roque, "Soil structure changes induced by tillage systems," Soil Tillage Res. **165**, 66–79 (2017). https://doi.org/10.1016/j.still.2016.07.010
72. L. F. Pires, W. L. Roque, J. A. Rosa, and S. J. Mooney, "3D analysis of the soil porous architecture under long term contrasting management systems by X-ray computed tomography," Soil Tillage Res. **191**, 197–206 (2019). https://doi.org/10.1016/j.still.2019.02.018
73. L. Pogosyan, K. Abrosimov, K. Romanenko, J. Marquez, and S. Sedov, "How is the fragipan incorporated in the pore space architecture of a boreal retisol?" Soil Res. **57** (6), 566–574 (2019). https://doi.org/10.1071/SR18239
74. L. Pogosyan, A. Gastelum, B. Prado, J. Marquez, K. Abrosimov, K. Romanenko, and S. Sedov, "Morphogenesis and quantification of the pore space in a

tephra-palaeosol sequence in Tlaxcala, central Mexico," Soil Res. **57** (6), 559–565 (2019). https://doi.org/10.1071/SR18185

75. V. Pot, X. Zhong, and P. C. Baveye, "Effect of resolution, reconstruction settings, and segmentation methods on the numerical calculation of saturated soil hydraulic conductivity from 3D computed tomography images," Geoderma **362**, 114089 (2020).
76. M. Prodanović and S. L. Bryant, "A level set method for determining critical curvatures for drainage and imbibition," J. Colloid Interface Sci. **304** (2), 442–458 (2006).
77. E. Rabot, M. Wiesmeier, S. Schlüter, and H.-J. Vogel, "Soil structure as an indicator of soil functions: a review," Geoderma **314**, 122–137 (2018).
78. A. Q. Raeini, B. Bijeljic, and M. J. Blunt, "Generalized network modeling: Network extraction as a coarse-scale discretization of the void space of porous media," Phys. Rev. E **96** (1), 013312 (2017).
79. A. Q. Raeini, M. J. Blunt, and B. Bijeljic, "Modeling two-phase flow in porous media at the pore scale using the volume-of-fluid method," J. Comput. Phys. **231**, 5653–5668 (2012).
80. P. Renard and D. Allard, "Connectivity metrics for subsurface flow and transport," Adv. Water Res. **51**, 168–196 (2013). https://doi.org/10.1016/j.advwatres.2011.12.001
81. M. R. Rokhforouz and H. A. Akhlaghi Amiri, "Phase-field simulation of counter-current spontaneous imbibition in a fractured heterogeneous porous medium," Phys. Fluids **29** (6), 062104 (2017).
82. K. A. Romanenko, E. B. Skvortsova, and V. A. Rozhkov, "Form and orientation of soil pores as indicators of a structural soil organization," IOP Conf. Ser.: Earth Environ. Sci. **368**, 012041 (2019). https://doi.org/10.1088/1755-1315/368/1/012041
83. K. A. Romanenko, V. V. Rogov, A. V. Yudina, K. N. Abrosimov, E. B. Skvortsova, and A. N. Kurchatova, "Frozen soils and sediments microstructure x-ray tomography study: methods, approaches, perspectives," Dokuchaev Soil Bull. **83**, 103–117 (2016). https://doi.org/10.19047/0136-1694-2016-83-103-117
84. T. Romanis, S. Sedov, S. Lev, M. Lebedeva, K. Kondratev, A. Yudina, K. Abrosimov, A. Golyeva, and D. Volkov, "Landscape change and occupation history in the Central Russian Upland from Upper Palaeolithic to medieval: paleopedological record from Zaraysk Kremlin," Catena **196**, 104873 (2021). https://doi.org/10.1016/j.catena.2020.104873
85. V. A. Rozhkov, *Soil Informatics* (Agropromizdat, Moscow, 1989) [in Russian].
86. V. Shabro, C. Torres-Verdín, F. Javadpour, and K. Sepehrnoori, "Finite-difference approximation for fluid-flow simulation and calculation of permeability in porous media," Transp. Porous Media **94**, 775–793 (2012). https://doi.org/10.1007/s11242-012-0024-y
87. F. San José Martínez, F. J. Muñoz Ortega, F. J. Caniego Monreal, A. N. Kravchenko, and W. Wang, "Soil aggregate geometry: measurements and morphology," Geoderma **237–238**, 36–48 (2015). https://doi.org/10.1016/j.geoderma.2014.08.003
88. A. Y. Sasov, "The investigation of the microstructure of soils by computed tomography," Vestn. Mosk. Univ., Ser. Geol. **3**, 56–62 (1987).
89. S. Schlüter, C. Großmann, J. Diel, G.-M. Wu, S. Tischer, A. Deubel, and J. Rücknagel, "Long-term effects of conventional and reduced tillage on soil structure, soil ecological and soil hydraulic properties," Geoderma **332**, 10–19 (2018). https://doi.org/10.1016/j.geoderma.2018.07.001
90. S. Schlüter, U. Weller, and H.-J. Vogel, "Segmentation of X-ray microtomography images of soil using gradient masks," Comput. Geosci. **36** (10), 1246–1251 (2010).
91. S. Schlüter, U. Weller, and H.-J. Vogel, "Soil-structure development including seasonal dynamics in a long-term fertilization experiment," J. Plant Nutr. Soil Sci. **174**, 395–403 (2011). https://doi.org/10.1002/jpln.201000103
92. E. V. Shein, E. B. Skvortsova, A. V. Dembovetskii, K. N. Abrosimov, L. I. Il'in, and N. A. Shnyrev, "Pore-size distribution in loamy soils: a comparison between microtomographic and capillarimetric determination methods," Eurasian Soil Sci. **49**, 315–325 (2016). https://doi.org/10.1134/S1064229316030091
93. E. B. Skvortsova, E. V. Shein, K. N. Abrosimov, K. M. Gerke, D. V. Korost, K. A. Romanenko, V. S. Belokhin, and A. V. Dembovetskii, "Tomography in soil science," Dokuchaev Soil Bull. **86**, 28–34 (2016). https://doi.org/10.19047/0136-1694-2016-86-28-34
94. A. S. Sorokin, K. N. Abrosimov, M. P. Lebedeva, and G. S. Kust, "Composition and structure of aggregates from compacted soil horizons in the southern steppe zone of European Russia," Eurasian Soil Sci. **49**, 326–337 (2016). https://doi.org/10.1134/S1064229316030108
95. A. V. Suzdaleva, E. V. Shein, N. V. Verkhovtseva, and K. N. Abrosimov, "Physical and microbiological aspects of the soil seedbed in the early formation of the barley root system (*Hordeum vulgare* L.): tomographic studies," IOP Conf. Ser.: Mater. Sci. Eng. **941**, 012032 (2020). https://doi.org/10.1088/1757-899X/941/1/012032
96. C. O. Tan, D. Kuppens, and R. Gupta, "Dual-energy CT," in *Neuroimaging Techniques in Clinical Practice: Physical Concepts and Clinical Applications* (Springer-Verlag, Cham, 2020). https://doi.org/10.1007/978-3-030-48419-4_7
97. E. W. Tollner and C. Murphy, "Factors affecting soil x-ray absorption coefficients with computer tomography," Am. Soc. Agric. Eng. **34** (3), 1047–1053 (1991).
98. S. Torquato, *Random Heterogeneous Materials: Microstructure and Macroscopic Properties* (Springer-Verlag, New York, 2002).
99. J. K. Torrance, T. Elliot, R. Martin, and R. J. Heck, "X-ray computed tomography of frozen soil," Cold Reg. Sci. Technol. **53**, 75–82 (2008).
100. R. A. Victor, M. Prodanović, and C. Torres-Verdín, "Monte Carlo approach for estimating density and

atomic number from dual-energy computed tomography images of carbonate rocks," J. Geophys. Res.: Solid Earth **122** (12), 9804–9824 (2017).

101. H.-J. Vogel, "Morphological determination of pore connectivity as a function of pore size using serial sections," Eur. J. Soil Sci. **48**, 365–377 (1997). https://doi.org/10.1111/j.1365-2389.1997.tb00203.x
102. H.-J. Vogel, "Topological characterization of porous media," in *Morphology of Condensed Matter: Physics and Geometry of Spatially Complex Systems* (Springer-Verlag, Berlin, 2002), pp. 75–92.
103. H.-J. Vogel, U. Weller, and S. Schlüter, "Quantification of soil structure based on Minkowski functions," Comput. Geosci. **36**, 1236–1245 (2010). https://doi.org/10.1016/j.cageo.2010.03.007
104. IUSS Working Group WRB, *World Reference Base for Soil Resources 2014, International Soil Classification System for Naming Soils and Creating Legends for Soil Maps, World Soil Resources Reports No. 106* (UN Food and Agriculture Organization, Rome, 2014).
105. Y. S. Yang, K. Y. Liu, S. Mayo, A. Tulloh, M. B. Clennell, and T. Q. Xiao, "A data-constrained modeling approach to sandstone microstructure characterization," J. Petrol. Sci. Eng. **105**, 76–83 (2013).
106. A. V. Yudina and K. A. Romanenko, "Mechanistic understanding of soil hierarchical structure," in *Proceedings of the EGU General Assembly* (Vienna, 2019). https://doi.org/10.13140/RG.2.2.26167.16809
107. Z. Zhang, K. Liu, H. Zhou, H. Lin, D. Li, and X. Peng, "Three-dimensional characteristics of biopores and non-biopores in the subsoil respond differently to land use and fertilization," Plant Soil **428**, 453–467 (2018). https://doi.org/10.1007/s11104-018-3689-3

Translated by D. Konyushkov